

# Comparing HARPS and Kepler surveys: On the alignment of multiple-planet systems

P. Figueira<sup>1</sup>, M. Marmier<sup>2</sup>, G. Boué<sup>1</sup>, C. Lovis<sup>2</sup>, N. C. Santos<sup>1,3</sup>, M. Montalto<sup>1</sup>, S. Udry<sup>2</sup>, F. Pepe<sup>2</sup>, and M. Mayor<sup>2</sup>

<sup>1</sup> Centro de Astrofísica, Universidade do Porto, Rua das Estrelas, 4150-762 Porto, Portugal  
e-mail: pedro.figueira@astro.up.pt

<sup>2</sup> Observatoire Astronomique de l'Université de Genève, 51 Ch. des Maillettes, - Sauverny - CH1290, Versoix, Suisse

<sup>3</sup> Departamento de Física e Astronomia, Faculdade de Ciências, Universidade do Porto, Portugal

## ABSTRACT

**Context.** The recent results of the HARPS and Kepler surveys provided us with a bounty of extrasolar systems. While the two teams analyzed extensively each of their data-sets, little work has been done comparing the two.

**Aims.** We study a subset of the planetary population whose characterization is simultaneously within reach of both instruments. We compare the statistical properties of planets in systems with  $m \sin i > 5-10 M_{\oplus}$  and  $R > 2 R_{\oplus}$ , as inferred from HARPS and Kepler surveys, respectively. If we assume that the underlying population has the same characteristics, the different detection sensitivity to the orbital inclination relative to the line of sight allows us to probe the planets' mutual inclination.

**Methods.** We considered the frequency of systems with one, two and three planets as dictated by HARPS data. We used Kepler's planetary period and host mass and radii distributions (corrected from detection bias) to model planetary systems in a simple yet physically plausible way. We then varied the mutual inclination between planets in a system according to different prescriptions (completely aligned, Rayleigh distributions and isotropic) and compared the transit frequencies with one, two or three planets with those measured by Kepler.

**Results.** The results show that the two datasets are compatible, a remarkable result especially because there are no tunable knobs other than the assumed inclination distribution. For  $m \sin i$  cutoffs of  $7-10 M_{\oplus}$ , which are those expected to correspond to the radius cutoff of  $2 R_{\oplus}$ , we conclude that the results are better described by a Rayleigh distribution with mode of  $1^{\circ}$  or smaller. We show that the best-fit scenario only becomes a Rayleigh distribution with mode of  $5^{\circ}$  if we assume a rather extreme mass-radius relationship for the planetary population.

**Conclusions.** These results have important consequences for our understanding of the role of several proposed formation and evolution mechanisms. They confirm that planets are likely to have been formed in a disk and show that most planetary systems evolve quietly without strong angular momentum exchanges such as those produced by Kozai mechanism or planet scattering.

**Key words.** (Stars:) Planetary systems, Techniques: radial velocities, photometric, Surveys, Methods: numerical, statistical

## 1. Introduction

We live very exciting times for extrasolar planet science. Since the first discovery of an extrasolar planet by Mayor & Queloz (1995), and thanks to the high efficiency of detection mechanisms, planetary detection rate has been increasing rapidly. As of today, more than 16 years past, we count  $\sim 700$  detected planets and many candidates to confirm. We have now both the data and the tools to explore the statistical properties of the planetary underlying population (e.g. Udry & Santos 2007).

From the technical perspective, during the last couple of years we have witnessed a spectacular increase in the precision (and consequently sensitivity) of the most efficient detection mechanisms. Using the radial velocity (RV) technique, the most efficient to date, the HARPS spectrograph detected 153 planets around G, K, and M stars, amongst which the lightest planets ever found, with a mass inferior to  $2 M_{\oplus}$  (Mayor et al. 2009; Lovis et al. 2011). The only spectrograph with demonstrated sub-m/s precision, HARPS allowed a detailed study of the underlying planetary population, yielding that at least 50% of the stars of the solar neighborhood have a planet orbiting around them with a period smaller than 100 days (Mayor et al. 2011).

As the Kepler mission became operational and the data were reduced, it became clear that the mission would set a new stan-

dard on photometric precision (Borucki et al. 2010). The candidate extrasolar planets revealed through the transit technique outnumbered those which had been found up to now, from ground or space. Out of the  $\sim 1250$  candidates found (Borucki et al. 2011)<sup>1</sup>, one can highlight the large number of extrasolar planet systems and the first secure confirmation of planets through transit timing variations (Lissauer et al. 2011a).

As information from the two surveys becomes available, a comparison between the results is warranted, and some authors started to tackle this problem (e.g. Wolfgang & Laughlin 2011). However, this task is complicated by several factors. The most obvious limitation is that these surveys rely on different techniques that probe different parameter's space. And, naturally, these techniques lead to different detection biases, providing two incomplete snapshots of the underlying population which only overlap partially, giving us a fragmented picture of the mass-radius diagram.

Particularly interesting is the dependence of both methods on orbital inclination relative to our line-of-sight. Planets transit

<sup>1</sup> Batalha et al. presented an updated planetary count of 2326 candidates at the Extreme Solar Systems II conference (09/2011), but since there was no official update on the planetary count, we will use the references cited instead.

only when their orbital movement makes them cover the disk of the star, as seen from our vantage point; this only happens close to our line-of-sight, restraining detections to small angles relative to it. On the other hand, RV techniques probe a much larger range of inclinations: in theory one can detect a system as long as its plane does not coincide with the plane of the sky; in practice the amplitude of the signal depends in a complex way on several orbital parameters, and its detectability is an even more complicated matter.

This has a particularly interesting consequence for planetary systems: while transit technique detects planetary systems which are not only aligned with our line of sight but close to coplanar, RV detects systems with a much higher inclination and consequently allows the detection of systems with a high mutual inclination between planets. In this work we propose a first comparison between planets from HARPS and Kepler surveys as a way of studying the mutual inclination between planets. We will restrict our analysis to planets with masses and radii within reach of the detection limits of both surveys in order to allow a simpler and more meaningful comparison.

In Sect. 2 we present an overview of the HARPS results of interest for our study and in Sect. 3 we describe our selection and analysis of the Kepler candidates. In Sect. 4 we describe the methodology that allows us to compare the planets from both surveys and present the results of this comparison. In Sect. 5 we discuss these results and conclude on Sect. 6.

## 2. The HARPS survey Results

The HARPS spectrograph (Mayor et al. 2003) has set a new benchmark in high-precision RV measurements, delivering several high-visibility results. Recently, Mayor et al. (2011) did a detailed statistical analysis of the volume-limited survey of HARPS+CORALIE and calculated the frequency of exoplanets with period up to 100 days, by calculating the detection limits for each star and correcting the measured planetary frequency from the detection bias. This analysis was done on a sample of 822 FGK stars, 376 of which are followed at a level allowing the detection of small-mass planets.

Of interest to us is a subset of the survey, for which comparison with Kepler is possible. We restrain our analysis to exoplanets defined by a mass cutoff whose RV signal makes the detection possible up to the largest period covered by Kepler analysis. This cutoff should be taken with care, since one cannot define *a priori* how large the  $K$  has to be relative to the instrumental precision for the planet to be detected in all the cases. Note that this ratio is non-constant and the reason why in order to evaluate the presence of planets on datasets one must resort to time-intensive Monte-Carlo analysis as those presented in Mayor et al. (2011).

In order to provide some latitude to our analysis and test the results for different mass-radius relationships, we repeat the analysis of Mayor et al. (2011) for different cutoffs: 5, 7, 9, and 10  $M_{\oplus}$  and for the periods between 0.68 and 50 days, the range of periods explored by Kepler. It is important to note that the detection probability of a 5  $M_{\oplus}$  planet in a 50 day orbit is already of 10-20 % (Fig. 7 of the paper); as a consequence the error bars on the corrected detection rates are quite large, making the results less constraining and less insightful. These mass cutoff values will turn out to be a very convenient choice, for a different reason, as discussed in the next Section.

The results for the true frequency of single planets and systems with two, three, and four planets are presented in Tab. 1. Note that these results are not corrected for  $\sin i$  selection effects.

This selection effect will bias the detections preferentially towards planets whose system's plane is closer to the line of sight. This might lead to an underestimation of the true frequency of planets, but in a way which is not a function of the number of planets in a system, but rather depends on the detectability of each planets' signal.

## 3. The Kepler mission Results

The Kepler photometric mission measured high-precision photometric variations of stellar flux on 160 000 stars (down to  $\sim 10$  ppm) and allowed (up to now) the detection of 1235 planet transit candidates (Borucki et al. 2011). Howard et al. (2011) did an extensive analysis of the published datasets and established the properties of the planetary population probed by the mission. Restricting the study to the subset of stars with high planet detectability, the authors quantified the planetary occurrence (as they named the true frequency of planets per star) as a function of planetary radius and period, from 0.68 to 50 days.

Of particular interest to us are planets with radii large enough for the planetary census to be considered complete and devoid of systematics, the threshold of which was defined as  $2 R_{\oplus}$  by the authors. Youdin (2011) repeated the analysis with a different methodology and, among many interesting results, confirmed this claim of completeness for at least  $R > 3 R_{\oplus}$ . Setting  $2 R_{\oplus}$  as the lower limit for data analysis makes the comparison with HARPS data easier, because according to Sotin et al. (2007) a planet with 10  $M_{\oplus}$  has a radius between 1.74 and 2.37  $R_{\oplus}$ .

Howard et al. (2011) presented the planet occurrence as the frequency of planets corrected from both geometrical probability and from the insufficient photometric precision. We repeated the same analysis, considering the same thresholds for detection but now separating planetary candidates into single planets, double transiting systems, triple transiting systems and quadruple transiting systems. All planetary and stellar parameters were extracted from the *Released Planet Kepler Candidates* list<sup>2</sup>. We considered the same candidates by imposing the same thresholds on Kepler star magnitude,  $T_{eff}$  and  $\log g$ , and setting the same S/N threshold on transit detection. When a system is composed of more than one planet we consider the photometric precision as dictated by the most stringent of the two planets, in line with what was done by Howard et al. (2011); in order to do so we consider the number of stars which still allow us to reach the required precision to detect both planets. We correct our planetary frequencies for the insufficient photometric precision but not for the transit probability. We do so because it is our objective to reproduce through simulations the frequency of planets that transit; these simulations include in a natural way the geometrical probability impact but cannot reproduce the effect of deficient photometric precision.

The frequency of single-transit planets, double transiting systems, triple transiting systems and quadruple transiting systems is presented in Tab. 2.

## 4. Comparing the Surveys

### 4.1. Methodology

The comparison of the results from the two methods is not straightforward. It is particularly difficult to match a cutoff in radius with one in mass. Here, by using different cutoff values we consider different mass-radius relationships. This relation is

<sup>2</sup> [http://archive.stsci.edu/kepler/planet\\_candidates.html](http://archive.stsci.edu/kepler/planet_candidates.html)

**Table 1.** The true frequency of single planets and systems with planetary periods between 0.68 and 50 days and  $m \sin i$  larger than 5, 7, 9, and 10  $M_{\oplus}$ , as calculated from HARPS data.

$m \sin(i)$	Single planets	Syst. w/ 2. plan.	Syst. w/ 3. plan.	Syst. w/ 4. plan.
$>5 M_{\oplus}$	$11.15 \pm 3.69 \%$	$4.63 \pm 2.27 \%$	$0.68 \pm 0.68 \%$	n.d.
$>7 M_{\oplus}$	$10.51 \pm 2.60 \%$	$2.19 \pm 1.26 \%$	n.d.	n.d.
$>9 M_{\oplus}$	$9.82 \pm 2.22 \%$	$1.21 \pm 0.85 \%$	n.d.	n.d.
$>10 M_{\oplus}$	$8.75 \pm 1.92 \%$	$0.57 \pm 0.57 \%$	n.d.	n.d.

n.d. stands for “not detected”; see Sect. 2 for more details.

**Table 2.** The transit frequency for planets and systems up to four planets with period between 0.68 and 50 days, as calculated from the Kepler candidates using the methodology from Howard et al. (2011).

Radii	Single transits	Double transits	Triple transits.	Quadruple transits
$>2R_{\oplus}$	5.23e-1 %	5.97e-2 %	9.26e-3 %	5.51e-3 %

n.d. stands for “not detected”; see Sect. 3 for more details.

not only unknown, but hardly unique, due to the different possible composition of exoplanets for the mass range considered (e.g. Valencia et al. 2007).

Starting from the observed HARPS frequencies stated above, we simulated systems whose inclination between the planets and the system’s (fixed) plane was controlled by tunable knobs. It is important to note that we considered planet frequencies as fixed (here used in plural because one must distinguish the frequency of stars with 1, 2, or 3 planets<sup>3</sup>). These were dictated by HARPS results and only depend on the mass cutoff (i.e. the mass-radius relationship assumed). The methodology is depicted in the flowchart presented in Fig. 1 and can be summarized in the following way:

- we created  $10^8$  planetary systems; the number of planets in each system was dictated by the frequencies of stars with one, two or three planets set by HARPS results.
- for each system the stellar radius is drawn from Kepler’s radius distribution of host stars. Each planet period  $P_k$  is drawn from the measured Kepler period distribution of planetary candidates.

The observed stellar radius distribution and planetary period distribution were corrected both from photometric detectability bias and from geometry bias. The geometry bias is corrected simply by applying the formula of the transit probability (e.g. Youdin 2011)

$$P_{\text{transit}} = 0.051 \left( \frac{10 \text{ days}}{P} \right)^{2/3} \left( \frac{\rho_{\odot}}{\rho_*} \right)^{1/3} \quad (1)$$

in which  $\rho$  is the mean stellar density and is valid for the cases of  $R_p \ll R_*$  and  $e = 0$ <sup>4</sup>. The photometric detectability bias, as corrected by Howard et al. (2011) reduces the accuracy of our measurements because it is presented for binned data in the  $(\log P, \log R_p)$  space. In order to correct for this last effect we use instead the power-law formulas (4), (5), and (6) of Youdin (2011). The interested reader is referred to this work for the details on the advantages of the approach.

<sup>3</sup> In principle, there is no reason not to consider the frequency of stars with higher number of planets around them; in practice these systems were not present in the sample studied.

<sup>4</sup> We consider that planetary orbits are circular, an hypotheses strengthened by the work of Moorhead et al. (2011), whom showed that Kepler transit durations imply a mean eccentricity  $\leq 0.2$ .

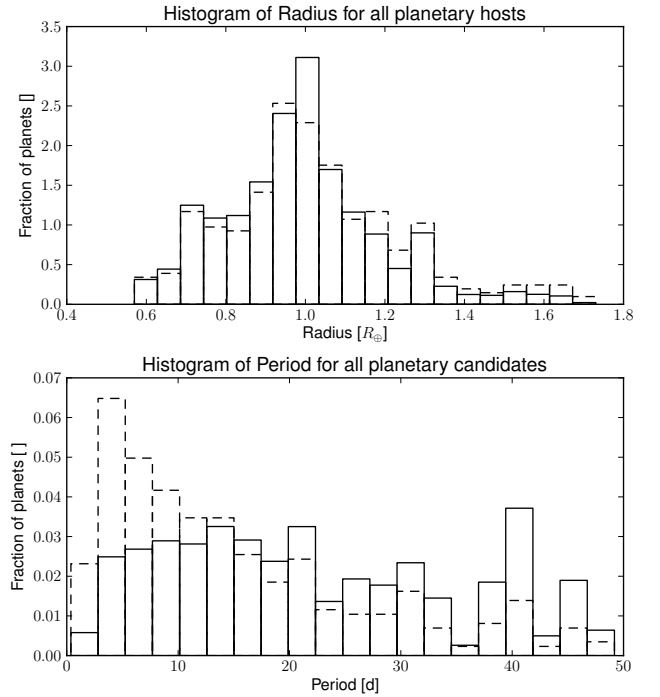


**Fig. 2.** Distribution of Radii for all Kepler planetary host (top) and Period for all Kepler planetary candidates considered for the  $2 R_{\oplus}$  radii cutoff (bottom); dashed histograms depict the distributions prior to the detection bias correction and solid line after.

We corrected for these two effects and only then binned the data into 20 equally sized bins and assigned a probability proportional to the (corrected) frequency of planets inside the bin; these distributions are presented in Fig. 2.

- For each drawn stellar radius, we draw a stellar mass with a flat probability between the extreme masses detected for the radii included in the bin. This allows us to translate orbital

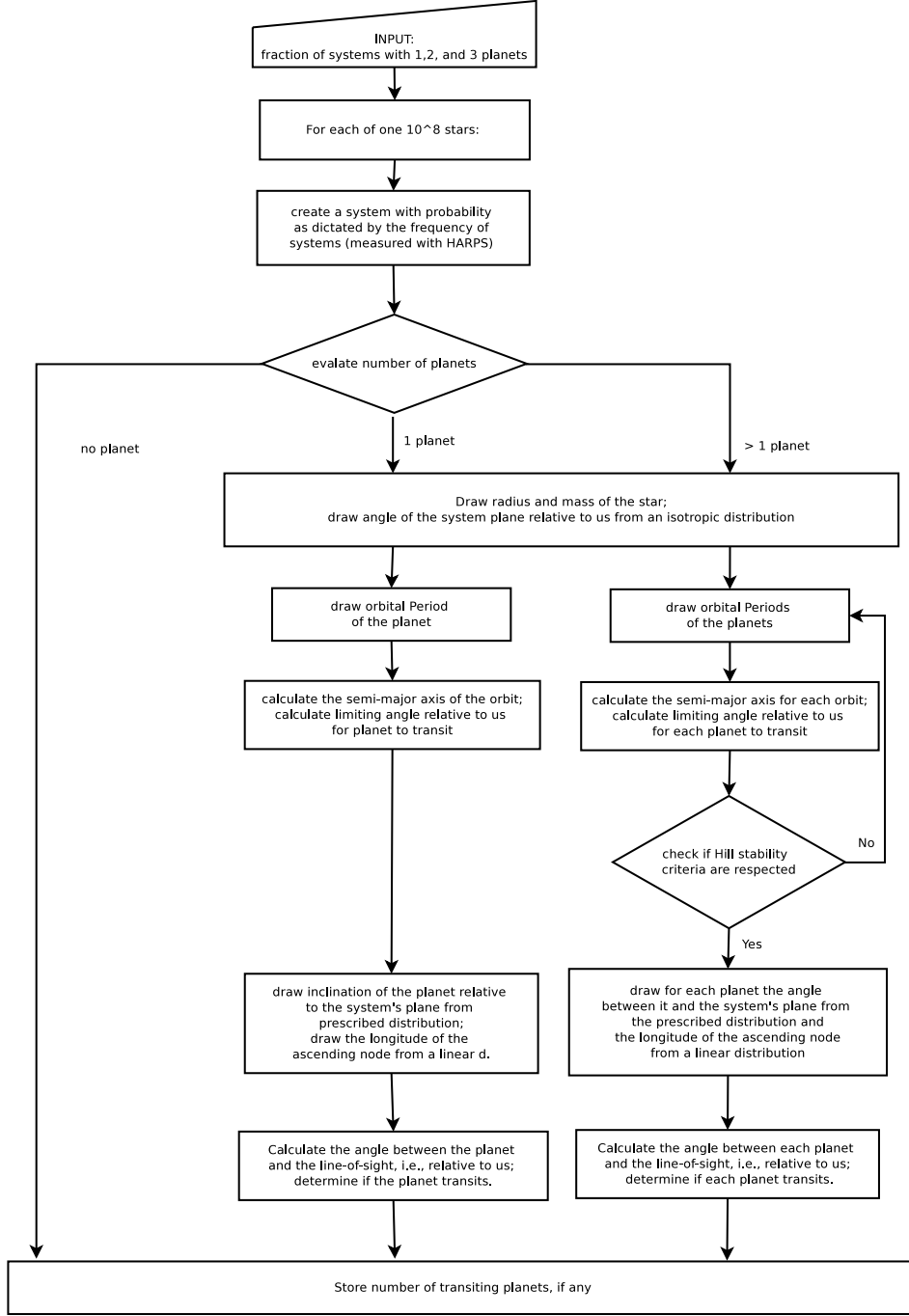


**Fig. 1.** Flowchart for the simulations described in Sect. 4.1.

periods  $P_k$  into orbital semi-major axis  $a_k$  using the generalized Kepler 3rd Law:

$$a_i = \sqrt[3]{\frac{M_*}{M_\odot} \frac{P^2}{1 \text{ yr}}} [A.U.]. \quad (2)$$

- If more than one planet is drawn for the system in question, the orbits have to respect the Hill stability criterion, as defined by Eq. (24) of Gladman (1993),

$$\frac{a_2 - a_1}{a_1} > 2.40 (\mu_1 + \mu_2)^{1/3} \quad (3)$$

in which  $\mu_1 = m_1/m_*$ ,  $\mu_2 = m_2/m_*$ . This equation is valid for circular orbits and when  $m_* \gg m_1, m_2$ . The planetary periods

are redrawn until all pairs of planets respect this property. We chose for  $m_1$  and  $m_2$  the  $m \sin i$  cutoff used for the considered HARPS frequency determination.

- The orientation of the system's plane relative to the line of sight plane,  $I$ , is drawn from a linear distribution in  $\sin$  (note that angles closer to the line of sight have a larger probability of being detected).
- For each planet the angle  $i_k$  with respect to the reference plane of the system is drawn from the assumed distribution (see next sub-section), and the longitude of the ascending node  $\Omega_k$  is drawn from a linear distribution between 0 and  $360^\circ$ .

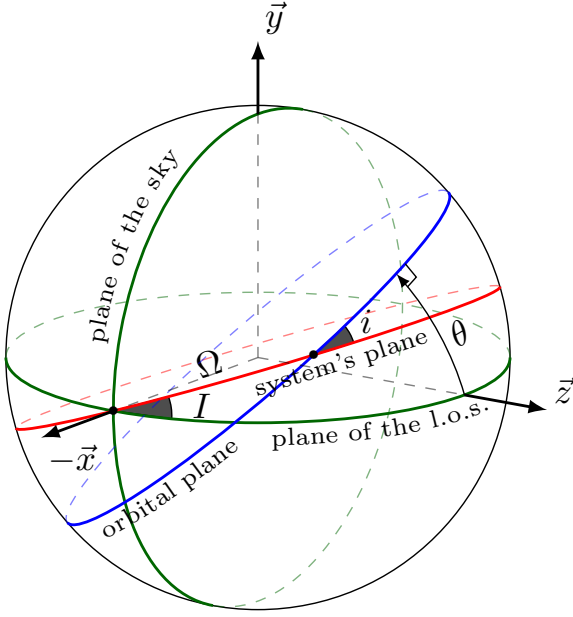


**Fig. 3.** Angles used in this paper. The observer is in the  $z$  direction.

- Finally, each angle  $\theta_k$  relative to the line of sight, as seen from our vantage point, is given by:

$$\theta_k = \arcsin |\cos I \cos \Omega \sin i + \sin I \cos i| \quad (4)$$

and the planet is considered to transit if  $\theta_k < \theta_{lim} = \arcsin(R_*/a_k)$ . The different planes and angles mentioned are depicted in Fig. 3.

It is important to note that we followed a methodology similar to that of Lissauer et al. (2011b), in which one starts from different primordial populations and tries to recover the frequency of observed Kepler transit candidates. However, in our case, and on top of several different minor aspects, we had a previously determined frequency of planets in systems for single planets, double-planet systems, and triple-planet systems. In order to estimate the error bars on our transit frequencies we used the  $1\text{-}\sigma$  uncertainties in HARPS frequencies to calculate extreme-case scenarios for the transit frequencies.

#### 4.2. Mutual inclination distributions & Results

For the distribution of the angles of each planet relative to the plane of the system  $i$  we considered 1) planets aligned with their systems plane; 2) different Rayleigh distributions  $R(\sigma)$  relative to the system's plane, where  $\sigma$ , the mode of the distribution, is the only governing parameter. For the latter we considered  $\sigma \in [1, 5, 10, 20, 30, 45]^\circ$ ; and 3) an isotropic distribution (i.e. a linear distribution in  $\cos i$ ). The results are presented in Tab. 3.

The obtained frequencies for single and double planetary transits are plotted and compared to those recovered from Kepler data in Fig 4. In this figure we plot in a 2-dimensions space the transit frequencies (and associated uncertainties) for single-transiting planets and double-transiting planets, as calculated from our simulations, for the different assumed inclinations (different panels) and different  $m \sin i$  cutoff (different markers and colors). On the same plot we present the values measured from Kepler data, so that both can be directly compared.

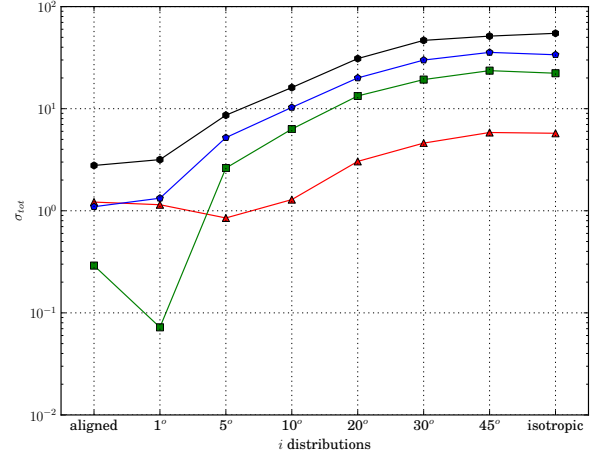


**Fig. 5.** The distance between Kepler point and the result from each simulation, measured in  $\sigma$ 's; the triangle, square, pentagon and hexagon (red, green, blue and black in electronic version only) represent the results for the 5, 7, 9 and  $10 M_\oplus$  cutoffs in  $m \sin i$ , respectively.

Note that for most cutoffs considered HARPS did not detect triple or quadruple systems for the given mass and period range. This was due to 1) the low number of stars surveyed when compared with Kepler's, for which the detection of a system with frequency of  $10^{-3}$  is quite low, and 2) to the low period range considered in the analysis, of 50 days. In fact, many of the systems detected by HARPS extend to more than 50 days, up to 100 days, and were naturally not included in the analysis.

## 5. Discussion

### 5.1. On the likeliness of different $i$ distributions

The first point to note is that the results show a remarkable agreement between the simulations based on HARPS frequencies and the Kepler measurements. This is worth noting, specially because our simulation procedure has no tunable knobs; no effort was made to match the calculated with the observed. The only free parameter is the inclination distribution, as described.

From Fig. 4 one can conclude that while all considered distributions reproduce the fraction of stars with one transiting planet inside or close to  $1\text{-}\sigma$  error bars, most underestimate the frequency of stars with two transiting systems. Of interest is to quantify the difference between the observed quantities and those reproduced through simulations. To do so we calculated for each case the absolute deviation between the observed and calculated values, taking as units the  $1\text{-}\sigma$  uncertainties (our proxy for the transit frequencies'  $\sigma$ ). The results are presented in Tab. 4 and in Fig. 5 we plotted the quadratic sum of the two absolute deviations  $\sigma_{tot} = \sqrt{\sigma_{f_1}^2 + \sigma_{f_2}^2}$ , as a function of the considered  $i$  distribution, for the different  $m \sin i$  cutoffs.

An inspection of the Tab. 4 and Fig. 5 shows that, in general, the more misaligned the planets (the larger the mode of the  $i$  distribution considered), the larger the deviation relative to the measured Kepler values. For cutoffs of 9 and  $10 M_\oplus$  this is exactly the case, but for cutoffs of 5 and  $7 M_\oplus$  the most probable distributions are not the aligned one but Rayleigh with modes of 1 and  $5^\circ$ , respectively. This brings back the question of the impact of the  $m \sin i$  cutoff on our results. We saw in Sect. 3 that

**Table 3.** Frequency of simulated transiting systems with 1,2, and 3 planets, for the different planetary frequencies of Tab.2

$m \sin i$ cutoff	distribution	Single planets [%]	Syst. w/ 2. plan. [%]	Syst. w/ 3. plan. [%]
5 $M_{\oplus}$	aligned	$5.97\text{e-}01^{+2.27\text{e-}01}_{-2.27\text{e-}01}$	$1.51\text{e-}01^{+7.80\text{e-}02}_{-7.79\text{e-}02}$	$1.93\text{e-}02^{+1.88\text{e-}02}_{-1.88\text{e-}02}$
5 $M_{\oplus}$	$R(1.0^\circ)$	$6.39\text{e-}01^{+2.52\text{e-}01}_{-2.50\text{e-}01}$	$1.38\text{e-}01^{+7.30\text{e-}02}_{-7.47\text{e-}02}$	$1.42\text{e-}02^{+1.41\text{e-}02}_{-1.37\text{e-}02}$
5 $M_{\oplus}$	$R(5.0^\circ)$	$8.18\text{e-}01^{+3.52\text{e-}01}_{-3.53\text{e-}01}$	$6.60\text{e-}02^{+4.10\text{e-}02}_{-4.02\text{e-}02}$	$2.31\text{e-}03^{+2.40\text{e-}03}_{-1.81\text{e-}03}$
5 $M_{\oplus}$	$R(10.0^\circ)$	$8.77\text{e-}01^{+3.93\text{e-}01}_{-3.90\text{e-}01}$	$3.81\text{e-}02^{+2.37\text{e-}02}_{-2.40\text{e-}02}$	$7.17\text{e-}04^{+6.53\text{e-}04}_{-2.17\text{e-}04}$
5 $M_{\oplus}$	$R(20.0^\circ)$	$9.14\text{e-}01^{+4.16\text{e-}01}_{-4.12\text{e-}01}$	$2.12\text{e-}02^{+1.33\text{e-}02}_{-1.35\text{e-}02}$	$2.05\text{e-}04^{+2.04\text{e-}04}_{-2.05\text{e-}04*}$
5 $M_{\oplus}$	$R(30.0^\circ)$	$9.25\text{e-}01^{+4.25\text{e-}01}_{-4.20\text{e-}01}$	$1.56\text{e-}02^{+9.80\text{e-}03}_{-1.01\text{e-}02}$	$1.07\text{e-}04^{+1.11\text{e-}04}_{-1.07\text{e-}04*}$
5 $M_{\oplus}$	$R(45.0^\circ)$	$9.29\text{e-}01^{+4.21\text{e-}01}_{-4.23\text{e-}01}$	$1.30\text{e-}02^{+8.10\text{e-}03}_{-8.54\text{e-}03}$	$6.30\text{e-}05^{+5.70\text{e-}05}_{-6.30\text{e-}05*}$
5 $M_{\oplus}$	isotropic	$9.30\text{e-}01^{+4.30\text{e-}01}_{-4.23\text{e-}01}$	$1.27\text{e-}02^{+8.30\text{e-}03}_{-8.18\text{e-}03}$	$6.90\text{e-}05^{+4.40\text{e-}05}_{-6.90\text{e-}05*}$
7 $M_{\oplus}$	aligned	$4.94\text{e-}01^{+1.39\text{e-}01}_{-1.40\text{e-}01}$	$6.75\text{e-}02^{+4.05\text{e-}02}_{-3.86\text{e-}02}$	n. d.
7 $M_{\oplus}$	$R(1.0^\circ)$	$5.13\text{e-}01^{+1.49\text{e-}01}_{-1.51\text{e-}01}$	$5.88\text{e-}02^{+3.39\text{e-}02}_{-3.38\text{e-}02}$	n. d.
7 $M_{\oplus}$	$R(5.0^\circ)$	$5.82\text{e-}01^{+1.91\text{e-}01}_{-1.91\text{e-}01}$	$2.38\text{e-}02^{+1.38\text{e-}02}_{-1.37\text{e-}02}$	n. d.
7 $M_{\oplus}$	$R(10.0^\circ)$	$6.03\text{e-}01^{+2.04\text{e-}01}_{-2.02\text{e-}01}$	$1.31\text{e-}02^{+7.40\text{e-}03}_{-7.64\text{e-}03}$	n. d.
7 $M_{\oplus}$	$R(20.0^\circ)$	$6.15\text{e-}01^{+2.11\text{e-}01}_{-2.09\text{e-}01}$	$6.94\text{e-}03^{+3.96\text{e-}03}_{-3.92\text{e-}03}$	n. d.
7 $M_{\oplus}$	$R(30.0^\circ)$	$6.20\text{e-}01^{+2.13\text{e-}01}_{-2.13\text{e-}01}$	$5.15\text{e-}03^{+2.83\text{e-}03}_{-3.00\text{e-}03}$	n. d.
7 $M_{\oplus}$	$R(45.0^\circ)$	$6.22\text{e-}01^{+2.15\text{e-}01}_{-2.13\text{e-}01}$	$4.28\text{e-}03^{+2.35\text{e-}03}_{-2.45\text{e-}03}$	n. d.
7 $M_{\oplus}$	isotropic	$6.22\text{e-}01^{+2.12\text{e-}01}_{-2.14\text{e-}01}$	$4.09\text{e-}03^{+2.50\text{e-}03}_{-2.32\text{e-}03}$	n. d.
9 $M_{\oplus}$	aligned	$4.41\text{e-}01^{+1.14\text{e-}01}_{-1.14\text{e-}01}$	$3.77\text{e-}02^{+2.66\text{e-}02}_{-2.66\text{e-}02}$	n. d.
9 $M_{\oplus}$	$R(1.0^\circ)$	$4.52\text{e-}01^{+1.20\text{e-}01}_{-1.21\text{e-}01}$	$3.26\text{e-}02^{+2.28\text{e-}02}_{-2.29\text{e-}02}$	n. d.
9 $M_{\oplus}$	$R(5.0^\circ)$	$4.91\text{e-}01^{+1.46\text{e-}01}_{-1.50\text{e-}01}$	$1.34\text{e-}02^{+8.90\text{e-}03}_{-9.50\text{e-}03}$	n. d.
9 $M_{\oplus}$	$R(10.0^\circ)$	$5.02\text{e-}01^{+1.56\text{e-}01}_{-1.57\text{e-}01}$	$7.31\text{e-}03^{+5.09\text{e-}03}_{-5.12\text{e-}03}$	n. d.
9 $M_{\oplus}$	$R(20.0^\circ)$	$5.09\text{e-}01^{+1.60\text{e-}01}_{-1.62\text{e-}01}$	$3.87\text{e-}03^{+2.79\text{e-}03}_{-2.72\text{e-}03}$	n. d.
9 $M_{\oplus}$	$R(30.0^\circ)$	$5.10\text{e-}01^{+1.63\text{e-}01}_{-1.61\text{e-}01}$	$2.83\text{e-}03^{+1.90\text{e-}03}_{-2.00\text{e-}03}$	n. d.
9 $M_{\oplus}$	$R(45.0^\circ)$	$5.13\text{e-}01^{+1.62\text{e-}01}_{-1.65\text{e-}01}$	$2.37\text{e-}03^{+1.61\text{e-}03}_{-1.68\text{e-}03}$	n. d.
9 $M_{\oplus}$	isotropic	$5.11\text{e-}01^{+1.63\text{e-}01}_{-1.62\text{e-}01}$	$2.34\text{e-}03^{+1.70\text{e-}03}_{-1.69\text{e-}03}$	n. d.
10 $M_{\oplus}$	aligned	$3.81\text{e-}01^{+9.60\text{e-}02}_{-9.40\text{e-}02}$	$1.76\text{e-}02^{+1.79\text{e-}02}_{-1.71\text{e-}02}$	n. d.
10 $M_{\oplus}$	$R(1.0^\circ)$	$3.86\text{e-}01^{+9.90\text{e-}02}_{-1.01\text{e-}01}$	$1.55\text{e-}02^{+1.55\text{e-}02}_{-1.50\text{e-}02}$	n. d.
10 $M_{\oplus}$	$R(5.0^\circ)$	$4.03\text{e-}01^{+1.19\text{e-}01}_{-1.16\text{e-}01}$	$6.04\text{e-}03^{+6.26\text{e-}03}_{-5.54\text{e-}03}$	n. d.
10 $M_{\oplus}$	$R(10.0^\circ)$	$4.08\text{e-}01^{+1.24\text{e-}01}_{-1.22\text{e-}01}$	$3.43\text{e-}03^{+3.50\text{e-}03}_{-2.93\text{e-}03}$	n. d.
10 $M_{\oplus}$	$R(20.0^\circ)$	$4.13\text{e-}01^{+1.26\text{e-}01}_{-1.27\text{e-}01}$	$1.85\text{e-}03^{+1.87\text{e-}03}_{-1.35\text{e-}03}$	n. d.
10 $M_{\oplus}$	$R(30.0^\circ)$	$4.13\text{e-}01^{+1.28\text{e-}01}_{-1.27\text{e-}01}$	$1.36\text{e-}03^{+1.25\text{e-}03}_{-8.60\text{e-}04}$	n. d.
10 $M_{\oplus}$	$R(45.0^\circ)$	$4.14\text{e-}01^{+1.26\text{e-}01}_{-1.27\text{e-}01}$	$1.12\text{e-}03^{+1.14\text{e-}03}_{-6.20\text{e-}04}$	n. d.
10 $M_{\oplus}$	isotropic	$4.14\text{e-}01^{+1.29\text{e-}01}_{-1.27\text{e-}01}$	$1.13\text{e-}03^{+1.07\text{e-}03}_{-6.30\text{e-}04}$	n. d.

The error bars were drawn from the lower and upper limit of HARPS frequencies uncertainties. n.d. stands for “not detected”; see Sect. 4 for more details. Note that for very small frequency values (marked with a \*), smaller than  $5\text{e-}04\%$ , the number of events is so low that the error bars are ill defined through Monte-Carlo analysis and cannot be considered meaningful.

**Table 4.** The absolute deviation between the Kepler transit frequencies for single and double transit systems for the  $2R_{\oplus}$  cutoff and those obtained through simulation in this paper (presented in Tab. 3), for the different assumed inclination distributions.

$i$ dist.	O-C( $5 M_{\oplus}$ )		O-C( $7 M_{\oplus}$ )		O-C( $9 M_{\oplus}$ )		O-C( $10 M_{\oplus}$ )	
	$\sigma_{f_1}$	$\sigma_{f_2}$	$\sigma_{f_1}$	$\sigma_{f_2}$	$\sigma_{f_1}$	$\sigma_{f_2}$	$\sigma_{f_1}$	$\sigma_{f_2}$
aligned	0.33	1.17	0.21	0.20	0.72	0.83	1.48	2.35
$R(1.0^\circ)$	0.46	1.05	0.07	0.03	0.59	1.19	1.38	2.85
$R(5.0^\circ)$	0.84	0.16	0.31	2.60	0.22	5.20	1.01	8.57
$R(10.0^\circ)$	0.91	0.91	0.40	6.30	0.13	10.29	0.93	16.08
$R(20.0^\circ)$	0.95	2.89	0.44	13.32	0.09	20.01	0.87	30.94
$R(30.0^\circ)$	0.96	4.50	0.46	19.28	0.08	29.93	0.86	46.67
$R(45.0^\circ)$	0.96	5.77	0.46	23.58	0.06	35.61	0.87	51.39
isotropic	0.96	5.66	0.46	22.24	0.07	33.74	0.84	54.74

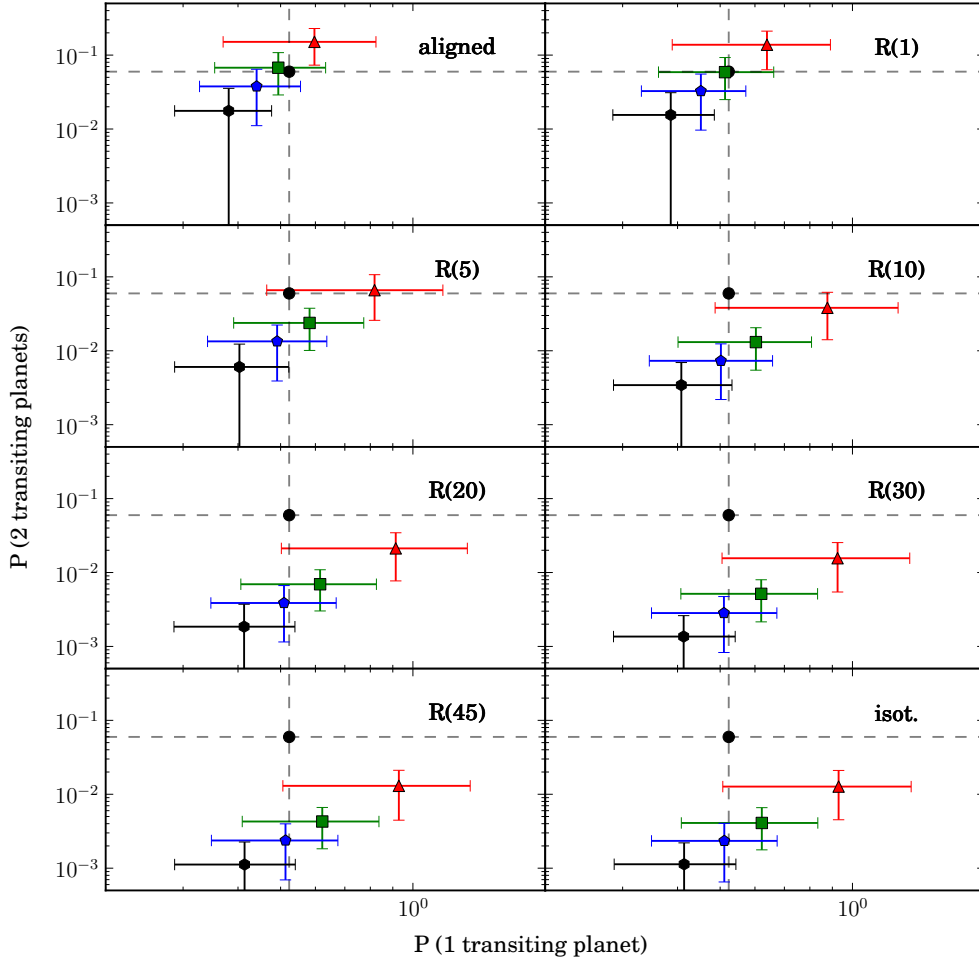


**Fig. 4.** Result of the simulations with the methodology described in 4.1 for the different  $i$  distributions considered.

The figure depicts the match between the frequency of single and double transiting systems obtained from our simulations and Kepler results. In each plot the black circle represents Kepler results and the triangle, square, pentagon and hexagon (red, green, blue and black in electronic version only) represent the results for the 5, 7, 9 and  $10 M_{\oplus}$  cutoffs in  $m \sin i$ ; the error bars result from the application of the  $1-\sigma$  uncertainties. The different sub-panels represent the application of different  $i$  distributions, from left to right and top to bottom: aligned,  $R(1^\circ)$ ,  $R(5^\circ)$ ,  $R(10^\circ)$ ,  $R(20^\circ)$ ,  $R(30^\circ)$ ,  $R(45^\circ)$  and isotropic, respectively.

a  $2 R_{\oplus}$  radius corresponds to a mass cutoff of around  $10 M_{\oplus}$ , of which precise value depends on the composition of the planets. We also know that by using  $m \sin i$  as a proxy for the real mass, we are underestimating the mass by a factor of 0.73, the average value of the  $\sin i$  for an isotropic distribution. So for the  $m \sin i$  cutoffs of 5, 7, 9, and 10, we are considering (in average) mass cutoff values of 6.3, 8.9, 11.4, and  $12.7 M_{\oplus}$ , respectively. At face value, this means that the results for  $m \sin i$  of 7 and  $9 M_{\oplus}$  are those that better match the cutoff in mass; interestingly, the result for the  $m \sin i$  cutoff of  $7 M_{\oplus}$  provides indeed the best match, and twice as close to Kepler’s measured values than the second best. However, the question is more involved than that: the span in composition means that a planet with mass lower by a couple of % than the average mass cutoff has a non-zero probability of having a radius above the cutoff. This sends a clear warning about matching a sharp cutoff in mass with one in radius.

It is thus important to note that only in the case of an extreme choice of mass cutoff we have the (relatively) high Rayleigh mode of  $5^\circ$  as the best match. As we saw before, one would have to assume a mass cutoff significantly lower than  $8.9 M_{\oplus}$  and closer to  $6.3 M_{\oplus}$ , which is at odds with the structure model’s results presented. According to Sotin et al. (2007) a planet with mass of  $6.3 M_{\oplus}$  has a radius between  $1.66$  and  $2.09 R_{\oplus}$ , for a water content of  $<0.1\%$  and  $\sim 50\%$ , respectively. This shows that planets with such mass are indeed too small to be included, or at least to contribute significantly for the population we recover by imposing as limiting radius  $2 R_{\oplus}$ . The only exception is the case of strongly irradiated planets, as discussed by Rogers et al. (2011), for which, under very strong irradiation ( $500 < T_{\text{eff}} < 1000$  K) and other assumptions, a planet with mass as low as  $4 M_{\oplus}$  can have a radius large enough to be included in our cutoff. However, once again, it is unlikely that these planets dominate our population.



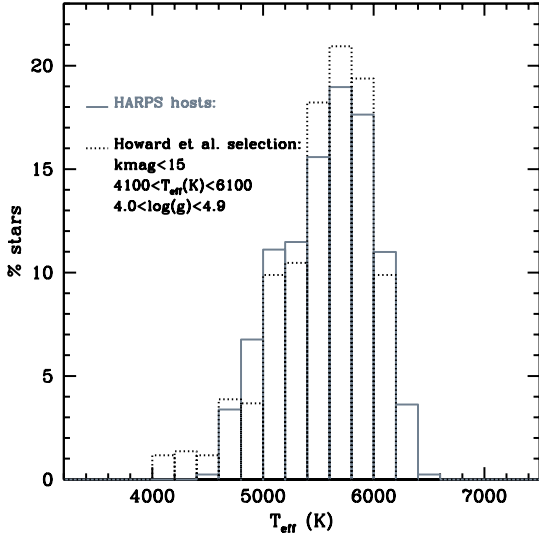


**Fig. 6.** Histogram of Kepler stars selected by effective temperature, from 3000 to 7500 K in bins of 200 K. In grey and with a solid line we present HARPS host and in black with a dotted line we present stars selected from the Kepler candidate stars which respected Howard et al. (2011) selection criteria (and are thus eligible for further planetary detection).

It is important to note that Eq. 3 is only valid for coplanar systems. Multi-planetary systems with relative inclinations larger than zero have more degrees of freedom and are thus more easily unstable. Then, stability should require larger planet separations. Nevertheless, in this study we chose to treat all the systems in the same way to avoid any uncontrolled bias. Since planets on wider orbits have lower transit probabilities, our choice increases slightly the transit probability of the outer planets of non-coplanar systems. The same argument can be used to show that if larger masses are used in the calculation of the Hill stability criterion, the spacing between the planets is increased and the transit probability decreased. Unfortunately, due to the lack of appropriate stability studies for inclined systems, one cannot do better than is done here.

We can then conclude that the inclination distribution that better reproduces Kepler single and double-transit frequencies follow a Rayleigh distribution with mode of  $\sim 1^\circ$  or even smaller, but we caution that the limitations of the approach presented here lead more to an order-of-magnitude result than to a clearly defined value. What can be asserted from our analysis is that a Rayleigh distribution with a mode of  $5^\circ$  can only be accommodated if we consider a population characterized by an extreme mass-radius relationship that would lead to very light planets ( $\sim 6 M_\oplus$ ) having typically a radius larger than  $2 R_\oplus$ .

## 5.2. On the impact of different stellar hosts: spectral types and metallicity

When comparing the different surveys outcome, one must take into account that the population of stars surveyed even though similar, has different characteristics. The first point to evaluate is the spectral type of the hosts themselves, since planetary formation is expected to be a function of stellar mass (e.g. Alibert et al. 2011), among other parameters.

In Fig. 6 we over-plot the two  $T_{\text{eff}}$  distributions obtained from HARPS and Kepler hosts considered in this study. We notice that Kepler host temperatures extend up to 400 K cooler than the coolest HARPS hosts, and conversely HARPS hosts extend to 400 K hotter than the hottest Kepler hosts. Both distributions have their peak around 5700 K, but the Kepler distribution is more peaked while HARPS is wider.

The  $T_{\text{eff}}$  determination of HARPS data was done as described by the calibration of Sousa et al. (2008) and its internal accuracy is of 50 K. The accuracy of the effective temperatures given by the Kepler Input Catalog (KIC) was estimated to be within 200 K for stars in the range between 4500 K and 6500 K (Brown et al. 2011). Recently, systematic differences between the *griz* magnitudes and those of the SDSS (DR8) have been noticed (Pinsonneault et al. 2011). Comparisons of (J-Ks)-based temperatures from the Infrared Flux Method (IRFM) and SDSS filter indicated a mean shift towards hotter temperatures with respect to the KIC of order 215 K in between 4000 K and 6500 K. This result seems to be confirmed also by high precision spectroscopic measurements. Metcalfe et al. (2010) determined the effective temperature of the sun-like star KIC11026764 by means of several spectroscopic approaches. They determined that this object is typically 100 K and 300 K hotter than the value reported in the KIC, which is in line with the possible offset between our two distributions.

Another possible bias in our comparison may come from the different metallicity distribution of the HARPS and Kepler samples. On the one side, all HARPS stars are in the solar neighborhood (closer than 50 pc), the vast majority of which belonging to the galactic thin disk. On the other side, Kepler targets are all much farther away (no longer solar neighborhood objects). Adding to this, Kepler targets are slightly above the galactic plane (Howard et al. 2011), suggesting that they may be more metal poor (on average) than solar neighborhood stars due to a higher proportion of thick disk objects<sup>5</sup>. This may have important implications regarding the type of planets found in the two samples. For instance, it has been shown that giant planets are preferentially found around metal-rich stars (Santos et al. 2001, 2004; Fischer & Valenti 2005), while this same trend is not seen for neptunes and super-Earths (Udry & Santos 2007; Mayor et al. 2011; Sousa et al. 2011). The stellar metal content may also affect the stellar radius, since [Fe/H] correlates with stellar radius (Guillot et al. 2006). The impact of these effects is difficult to quantify; the two quantities are expected to be correlated. However, using the Besançon model, Howard et al. (2011) derived a  $\sim 0.1$  dex effect in [Fe/H] as a function of spectral type, a value that is not very pronounced.

The implications of these differences are far from obvious and its study requires a detailed knowledge of the impact of stellar host properties on planet formation – and eventually a more refined analysis of Kepler hosts parameters. This is far beyond the reach of this paper, and we will content ourselves with noting that the two populations do not seem to differ in a significant way.

## 5.3. Comparison with other works and consequences for formation and evolution mechanisms

Lissauer et al. (2011b) analyzed the architecture of Kepler planetary system candidates (i. e. the observed multiplicity frequencies) and concluded that a single population of planetary sys-

<sup>5</sup> Thick disk stars are more deficient on average than thin disk counterparts (e.g. Adibekyan et al. 2011).



tems which matched the higher multiplicities under-predicted the number of single-transiting systems. The authors provide also constraints on the frequency of systems with 1 to 6+ planets and mutual inclination, even though these two parameters are naturally correlated. However, their results were obtained using a methodology which required the normalization of the number of simulated transits to reproduce the total number of transits detected by Kepler, making it vulnerable to the presence of false planet positives (FPP). Morton & Johnson (2011), calculate a FPP rate  $< 10\%$  for 90% of all Kepler candidates, the average being closer to 5% and with tails extending up to 30%. The presence of FPP also has an impact on our study, since it will modify the planetary period distribution and stellar radii and mass distributions. However, and unlike Lissauer et al. (2011b), here the discrimination between the different models is made essentially through the frequency of double transiting extrasolar planets, for which the FPP is much lower than on average or for single-planet systems (Lissauer et al. 2012), which makes our results probably more robust.

Our work shows that planetary systems are likely to host planets with a very low inclination relative to the plane of the system. This is already the case for the Solar System, which has an average inclination  $< 2^\circ$ , and favors the standard model for planet formation in a disk. More importantly, it suggests that most planets in systems do not have their orbital elements influenced by violent angular momentum exchanges such as planet-planet scattering (e.g. Nagasawa et al. 2008), Kozai oscillation (e.g. Wu & Murray 2003) or perturbation by a stellar encounter (e.g. Malmberg et al. 2011), mechanisms which are only expected to create short-period single planets and not systems. As already pointed out by Greg Laughlin<sup>6</sup>, the distribution of orbital parameters for Kepler multi transit systems is very similar of that of the same (scaled) parameters for Solar System giant planet satellites. This is well in line with the fact the planets should be formed in a disk, with relative low orbital inclinations, as we show here.

## 6. Conclusions

We attempt at a first comparison between the planetary population properties as characterized by HARPS and Kepler surveys. We simulated the population of planets, with planetary frequencies dictated by HARPS survey results, and considered that these planets followed different inclination distributions relative to the systems' plane. We considered distributions from aligned to Rayleigh distributions with different modes, to finally isotropic (completely independent).

The first remarkable point is the compatibility of the results from the two surveys. This is made even more so by the very low freedom we have on influencing our simulations' outcome. There are no tunable knobs other than the inclination distribution. Concerning these, we showed that the results point to a strong alignment of the systems, with an inclination between the planet and the plane of the system which is better described by a Rayleigh distribution with mode of  $\sim 1^\circ$  or even smaller. This is a feature which depends on the assumed mass-radius relationship, but not in a strong way, an important point since the mass-radius relationship for low-mass planets is ill-defined and hardly unique, due to the span of compositions and mass which can generate the same radius. We have shown that only in extreme and

thus highly unlikely cases the best-fit for the alignment between planets is expected to follow a  $R(5^\circ)$ .

These results have important consequences for our understanding of the role of several proposed formation and evolution mechanisms. They confirm that planets are likely to have been formed in a disk and show that most planetary systems evolve quietly without strong angular momentum exchanges such as those produced by Kozai mechanism or planet scattering.

*Acknowledgements.* This work was supported by the European Research Council/European Community under the FP7 through Starting Grant agreement number 239953, as well as by Fundação para a Ciência e a Tecnologia (FCT) in the form of grant reference PTDC/CTE-AST/098528/2008. NCS would further like to thank FCT through program Ciência2007 funded by FCT/MCTES (Portugal) and POPH/FSE (EC). MM is supported by grant SFRH/BPD/71230/2010, from FCT (Portugal). PF would like to thank to Manuel Monteiro for his highly skilled and prompt assistance on running the simulations in a cluster.

## References

- Adibekyan, V. Z., Santos, N. C., Sousa, S. G., & Israelian, G. 2011, *A&A*, 535, L11
- Alibert, Y., Mordasini, C., & Benz, W. 2011, *A&A*, 526, A63+
- Borucki, W. J., Koch, D., Basri, G., et al. 2010, *Science*, 327, 977
- Borucki, W. J., Koch, D. G., Basri, G., et al. 2011, *ApJ*, 736, 19
- Brown, T. M., Latham, D. W., Everett, M. E., & Esquerdo, G. A. 2011, *AJ*, 142, 112
- Fischer, D. A. & Valenti, J. 2005, *ApJ*, 622, 1102
- Gladman, B. 1993, *Icarus*, 106, 247
- Guillot, T., Santos, N. C., Pont, F., et al. 2006, *A&A*, 453, L21
- Howard, A. W., Marcy, G. W., Bryson, S. T., et al. 2011, *ArXiv e-prints*
- Lissauer, J. J., Fabrycky, D. C., Ford, E. B., et al. 2011a, *Nature*, 470, 53
- Lissauer, J. J., Marcy, G. W., Rowe, J. F., et al. 2012, *ArXiv e-prints*
- Lissauer, J. J., Ragozzine, D., Fabrycky, D. C., et al. 2011b, *ApJS*, 197, 8
- Lovis, C., Ségransan, D., Mayor, M., et al. 2011, *A&A*, 528, A112
- Malmberg, D., Davies, M. B., & Hoggie, D. C. 2011, *MNRAS*, 411, 859
- Mayor, M., Marmier, M., Lovis, C., et al. 2011, *ArXiv e-prints*
- Mayor, M., Pepe, F., Queloz, D., et al. 2003, *The Messenger*, 114, 20
- Mayor, M. & Queloz, D. 1995, *Nature*, 378, 355
- Mayor, M., Udry, S., Lovis, C., et al. 2009, *A&A*, 493, 639
- Metcalf, T. S., Monteiro, M. J. P. F. G., Thompson, M. J., et al. 2010, *ApJ*, 723, 1583
- Moorhead, A. V., Ford, E. B., Morehead, R. C., et al. 2011, *ApJS*, 197, 1
- Morton, T. D. & Johnson, J. A. 2011, *ApJ*, 738, 170
- Nagasawa, M., Ida, S., & Bessho, T. 2008, *ApJ*, 678, 498
- Pinsonneault, M. H., An, D., Molenda-Žakowicz, J., et al. 2011, *ArXiv e-prints*
- Rogers, L. A., Bodenheimer, P., Lissauer, J. J., & Seager, S. 2011, *ApJ*, 738, 59
- Santos, N. C., Israelian, G., & Mayor, M. 2001, *A&A*, 373, 1019
- Santos, N. C., Israelian, G., & Mayor, M. 2004, *A&A*, 415, 1153
- Sotin, C., Grasset, O., & Mocquet, A. 2007, *Icarus*, 191, 337
- Sousa, S. G., Santos, N. C., Israelian, G., Mayor, M., & Udry, S. 2011, *A&A*, 533, A141
- Sousa, S. G., Santos, N. C., Mayor, M., et al. 2008, *A&A*, 487, 373
- Udry, S. & Santos, N. C. 2007, *ARA&A*, 45, 397
- Valencia, D., Sasselov, D. D., & O'Connell, R. J. 2007, *ApJ*, 665, 1413
- Wolfgang, A. & Laughlin, G. 2011, *ArXiv e-prints*
- Wu, Y. & Murray, N. 2003, *ApJ*, 589, 605
- Youdin, A. N. 2011, *ApJ*, 742, 38

<sup>6</sup> Oral communication at the "First Kepler Science Conference", December 2011.